ELSEVIER

Contents lists available at ScienceDirect

Optical Materials

journal homepage: www.elsevier.com/locate/optmat



Optical constants of titanium-doped gallium oxide thin films

Sandeep Manandhar, Anil K. Battu, Cristian Orozco, C.V. Ramana*

Center for Advanced Materials Research (CMR), University of Texas at El Paso, 500 W University Ave, El Paso, TX, 79968, USA



ARTICLE INFO

Keywords:
Ga₂O₃
Ti doping
Optical constants
Spectroscopic ellipsometry

ABSTRACT

This study explores the effect of titanium (Ti) doping on the optical constants of nanocrystalline gallium oxide (Ga_2O_3) films (GTO). Co-sputtering of the Ga_2O_3 and Ti targets with a variable sputtering power to Ti allowed the fabrication of GTO films with a variable Ti-content from 0 to ~ 5 at%. The optical constants, namely index of refraction (n) and extinction coefficient (k), and their dispersion profiles determined indicate that the n profiles are sensitive the Ti content while all the GTO films were transparent. The n values at 632 nm varies in the range of 1.78–1.84 due to gradual increase of Ti concentration from 0 to 5%. Lorentz-Lorenz analysis of the optical constants data indicates the gradual improvement in the packing density coupled with structural transformation accounts for the observed optical quality of the Ti-doped Ga_2O_3 films as a function of Ti concentration. A correlation between the material composition, Ti concentration and optical constants is discussed.

1. Introduction

Gallium oxide (Ga₂O₃), which is regarded as an ultra-wide band gap material, has been receiving recent attention of scientific and research community for its interesting physical, chemical and electronic properties, which can be readily utilized in numerous technological applications [1]. β-Ga₂O₃ based materials find technological applications in chemical sensors [2-4], magnetic memories [5], and solar-blind deep UV detectors [6,7]. Excellent, deep transparency in the ultraviolet (UV) region of the electromagnetic spectrum coupled with a wide band gap $(E_g \sim 4.8 \text{ eV})$ and high thermal stability of β -Ga₂O₃ makes it interesting for transparent electrodes in UV-based photovoltaics [8-10]. solarblind deep UV detenctors, optoelectronics [3,8,11,12], and luminescent displays [12]. The relatively large value of electric field breakdown field strength (8 MVcm⁻¹) makes β-Ga₂O₃ attractive choice for the design and development of high-power electronic devices [1]. However, a detailed fundamental understanding of the structure-optical property relationship is important for utilization of intrinsic and doped β-Ga₂O₃ thin films in all of the aforementioned device applications.

The properties and device applications of β -Ga₂O₃ can be tuned or controlled by doping with certain metal ions which can significantly alter the physical and electronic properties. From the view point of an optical material, efforts documented in the lietrature for doping of Sn, Cr, Cu, Ti, Mo and W into β -Ga₂O₃ suggest changes in the optical absorption and band gap [3,8,12–15]. Similarly, Sn- or Cr-doped Ga₂O₃ nanowires were shown to exhibit tailored properties for application in luminescent display devices [12]. Doping certain type of metal ions,

such as Ni, Zn, and Pb, enhances the photocatalytic activity of Ga₂O₃ [16-19]. The obvious relevance and impetus for the present work on Tidoped Ga₂O₃ films is derived from the following considerations. First of all, the efforts directed towards Ti-doped Ga2O3 films in the literature are meager; therefore, understanding the fundamental science of materials from the Ga-Ti-O system is most compelling. Also, from applied science perspective, understadning the effect of Ti-doping into Ga2O3 may enhance our ability to design and development of novel functional materials for optical, optoelectronic and photo-catalytic applications. Note that TiO2, similar to Ga2O3, has been widely used in solar cells, photo-catalysis, and chemical sensors. Therefore, a fundamental scientific understanding of either single phase or composite materials derived from Ga-Ti-O system may offer unique properties and phenomena useful for a wide range of optical and photo-catalytic applications. Previously, we demonstrated the direct relationship between the structure and band gap of Ti-incorporated Ga2O3 films in a communication [13]. However, a more detailed account of fundamental understanding of the structure-composition-optical constants relationship is quite important to understand the optical and electrical properties and also to establish a road-map for practical utilization of Tidoped Ga₂O₃ (GTO) films. Most importantly, determining the optical constants, namely index of refraction (n) and extinction coefficient (k), along with band gap (Eg) is important for UV-transparent oxides, such as Ga2O3 in this case. Furthermore, for thin films and nanomaterials, these optical characteristics are sensitive to the microstructure. Surface/interface structure, crystal quality, packing density, lattice parameters, and defect structure strongly influences the Optical parameters

E-mail address: rvchintalapalle@utep.edu (C.V. Ramana).

^{*} Corresponding author.

of thin films and nanomaterials. On the other hand, tailoring the optical constants and their dispersion profiles open the door for engineering modern electronic and optical devices. Therefore, in the present work, optical constants of sputter-deposited GTO thin films were evaluated using spectrscopic ellispometry, which allowed us probing the optical quality of the films as a function of Ti doping as presented and discussed in this paper.

2. Experimental details

Intrinsic and Ti-incorporated Ga₂O₃ nanocrystalline (nc) films (referred to as GTO hereafter) were deposited onto silicon (Si) (100) wafers by radio-frequency magnetron sputtering. All the substrates were thoroughly cleaned by ultrasonication using ethyl alcohol. The substrates were then dried with nitrogen and then introduced into the vacuum chamber Co-sputtering of the Ga₂O₃ (99.999%) and Ti (99.95%) targets (2 in. diameter; Plasmaterials Inc.) was performed to produce GTO films with a variable Ti content. The Ga₂O₃ and Ti targets were placed on 2-in. sputter guns, which were placed at 8 cm from the substrate. The base pressure was $\sim 10^{-6}$ Torr. A sputtering power of 25 W was initially applied to the targets while introducing high-purity argon (Ar) into the chamber to ignite the plasma. The sputtering power was then increased to the desired or set values for Ga2O3 and Ti targets, respectively.. A constant sputtering power of 100 W was maintained for the Ga₂O₃ target. The Ti-target sputtering power was varied in the range of $0-100\,\mathrm{W}$ to change the Ti concentration (x) in the films. The argon and oxygen flows were controlled using MKS mass flow meters. The reactive deposition atmosphere was achieved by flowing 30 sccm of argon and 10 sccm of oxygen through separate mass flow controllers. The working pressure of argon was held at 2.0 mTorr, corresponding to a constant pumping speed of 190 L/s, prior to the introduction of oxygen. A constant pumping speed was achieved by locking the position of the gate valve between the turbomolecular pump and the deposition chamber. The total working pressure and the corresponding oxygen partial pressure (PO2) were monitored using a capacitance manometer.

Before each deposition, the Ga_2O_3 target was pre-sputtered for $10\,\mathrm{min}$ with the shutter above the gun closed. The samples were deposited at substrate temperature (T_s) of $500\,^\circ\mathrm{C}$. This deposition temperature was optimum for producing nanocrystalline β -phase Ga_2O_3 films [13,20]. The substrates were heated by resistive heating, and the desired T_s was controlled by an Athena X25 controller. In all experiments, the deposition time was 3 h. The incorporation of Ti increases the film thickness continuously from 190 to 290 nm. This is expected because the Ga_2O_3 target is being sputtered at a constant power resulting in a constant thickness ($\sim 190\,\mathrm{nm}$) while the amount of Ti incorporation increases the overall material flow and thickness of the GTO samples. The characterization of the samples and related analyses conidered all these factors. The GTO sample identification numbers were generated based on the sputtering power applied to the Ti target.

The optical constants and surface/interface characteristics were probed by spectroscopic ellipsometry (SE), which measures the relative changes in the amplitude and phase of the linearly polarized monochromatic incident light upon oblique reflection from the sample surface. The experimental parameters obtained by SE are the angles Ψ (azimuth) and Δ (phase change), which were determined over the wavelength range of 200-1600 nm at 300 K in the air on a J. A. Woollam vertical variable-angle spectroscopic ellipsometer with computer controlled Berek wave plate compensator (J.A. Woollam Co, Lincoln, NE). The selected angles of incidence are 60°, 65°, and 70°. The ellipsometry data analysis was performed using commercially available WVASE32 software [21]. The optical properties of Ga₂O₃ and GTO films were evaluated using spectrophotometry measurements employing a Cary 5000 UV-vis-NIR double-beam spectrophotometer. GTO films deposited on quartz were used for spectrophotometry measurements. Theoretical details needed to understand how the optical properties were calculated using the experimental data (ellipsometry and spectrophotometry) are briefly presented in the following section.

3. Theory, model and calculations

Spectroscopic ellipsometry (SE), which is a nondestructive optical method, allows the determination of optical constants and microstructure of thin oxide films. The SE measured angles (Ψ , the azimuth and Δ , the phase change) are related to the sample microstructure and optical properties as defined by Refs. [22–25]:

$$\rho = \frac{R_p}{R_s} = \tan \Psi \exp(i\Delta) \tag{1}$$

where R_p and R_s are the complex reflection coefficients of the light polarized parallel and perpendicular to the plane of incidence, respectively. For data analysis, the Levenberg-Marquardt regression algorithm was used for minimizing the mean-squared error (MSE) [22]:

$$MSE = \frac{1}{2N - M} \sum_{i=1}^{n} \left[\left\{ \frac{(\Psi_{exp} - \Psi_{calc})}{\sigma_{\Psi_{i}}^{exp}} \right\}^{2} + \left\{ \frac{(\Delta_{exp} - \Delta_{calc})}{\sigma_{\Delta_{i}}^{exp}} \right\}^{2} \right]$$
(2)

where Ψ_{exp} , Ψ_{calc} , and Δ_{exp} , Δ_{calc} are the measured (experimental) and calculated ellipsometry functions, N is the number of measured Ψ , Δ pairs, M is the number of fitted parameters in the optical model, and σ are standard deviations of the experimental data points.

Extracting meaningful physical and surface/interface information from SE requires the construction of an optical model of the sample that generally accounts several distinct layers with individual optical dispersions. Interfaces between these layers are optical boundaries at which light is refracted and reflected per the Fresnel relations. Fig. 1 shows the stack model used to simulate the spectra for the purpose of determining the optical constants of GTO films. The model contains, from the top, Ti-doped $\rm Ga_2O_3$ film, $\rm SiO_2$ interface, and Si substrate. The fitting procedure also considered the surface and interface roughness for accuracy.

Spectrophotometry measurements allow to determining the optical transparency and band gap. The band gap calculations [2,3,13,15] were done using optical absorption coefficient, α , of the films that is evaluated using the relation:

$$\alpha = [1/t] \ln[T/(1-R)^2], \tag{3}$$

where T is the transmittance, R the reflectance and t the film thickness. The average film thickness values determined from both SEM and SE data were employed to obtain the optical absorption coefficient of GTO films. Further analysis of the optical spectra and calculations allow understanding the effect of Ti incorporation on the optical properties..

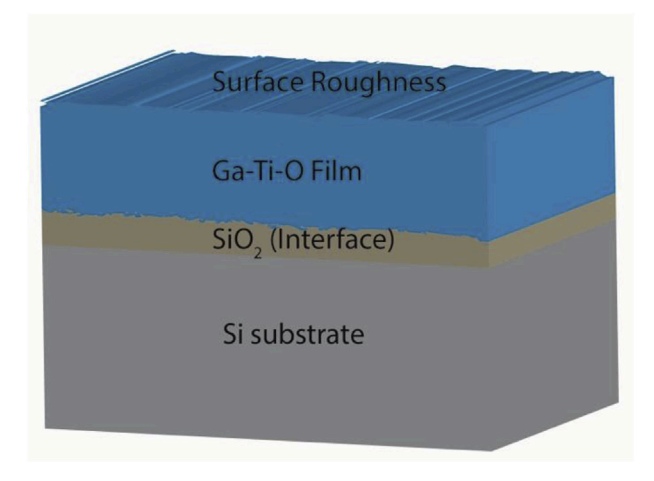


Fig. 1. Stack model of the GTO sample constructed for ellipsometry data analysis.

For β -Ga₂O₃ with a direct band gap [3,4,13,15] the absorption follows a power law of the form:

$$(\alpha h \nu) = B \left(h \nu - E_g \right)^{1/2} \tag{4}$$

where $h\nu$ is the energy of the incident photon, α is the absorption coefficient, B is the absorption edge width parameter, and E_g is the band gap. The details of spectrophotometry measurements and detailed analyses were reported elsewhere. However, comparison of the ellipsometry and spectrophotometry analyses made. Especially, the band gap values determined by these two methods are compared and validated.

4. Results and discussion

The Cauchy dispersion model was used since the GTO films are transparent in the respective wavelength region and also for other reason that it was successful to fit the data and explain the optical properties of intrinsic Ga_2O_3 films [26]. Also, this model was able to account for the optical properties of other wide band gap oxides such as La_2O_3 [27], Y_2O_3 [25], and HfO_2 [28,29]. The Cauchy equation for refractive index n as function of wavelength λ can be expressed as:

$$n(\lambda) = A + \frac{B}{\lambda^2} + \frac{C}{\lambda^4} \tag{5}$$

where A, B, and C are the Cauchy coefficients and specific to the material. A is the constant that dominates $n(\lambda)$ for long wavelengths, B controls the curvature of $n(\lambda)$ in the middle of the visible spectrum, and C influences the $n(\lambda)$ to the greater extent at shorter wavelengths. Also, the principle behind Cauchy's model can also be used for the dispersion function $k(\lambda)$:

$$k(\lambda) = d + \frac{e}{\lambda^2} + \frac{f}{\lambda^4} \tag{6}$$

where d, e and f are constants specific to the material [25,29,30]. Thus, the Cauchy model and fitting of the recorded experimental data allow for the optical constants (n and k) determination as well as thickness verification. The model/fitting parameters are presented in Table 1 while Fig. 2 shows the spectral dependencies of the SE functions, Ψ and Δ , determined for GTO films. The spectral dependencies of Ψ and Δ were fitted with appropriate models to extract film thickness and the optical constants, i.e., the refractive index (n) and extinction coefficient (k), based on the best fit between experimental and simulated spectra [22,23]. The curves obtained for Ti-doped Ga₂O₃ films indicate (Fig. 2) a reasonable agreement between the experimental and simulation data for the entire range of Ti-concentration.

The microstructure information, specifically, film thickness, roughness and interfacial oxide thickness of GTO films, was also obtained from SE analysis. The film thickness variation as a function of Ti sputtering power and/or Ti concentration is presented in Fig. 3. It is evident that the film thickness is steadily increasing with Ti sputtering power. Fig. 3 also, shows the variation of surface roughness of the Tidoped $\rm Ga_2O_3$ films determined from SE analysis.

The dispersion profiles of the index of refraction (n) determined from SE data for Ti-doped Ga_2O_3 films are shown in Fig. 4a. The 'n' dispersion profiles indicate a sharp increase at shorter wavelengths corresponding to fundamental absorption of energy across the band gap. The 'structure and Ti-content' dependence is evident in the dispersion curves (Fig. 4a), where a progressive increase of n value with increasing Ti content (Fig. 4b) is evident in GTO films. The spectral dependence of the extinction coefficient (k) determined from SE data for Ti-doped Ga_2O_3 films is shown in the insert of Fig. 4a. It is evident that the extinction coefficient values are low and very close to zero in most parts of the spectrum (insert, Fig. 4a) which indicates very low optical losses due to absorption. The onset or sharp increase in k at high photon energy or short wavelength is due to the fundamental absorption across the band gap. The dispersion profiles of $k(\lambda)$ reveal the structural quality of Ti-doped Ga_2O_3 films. Specifically, the curves

 $0.00076143 \pm 8.6183E-05$ 303.08 ± 1.423 0.00974 ± 0.00076516 1.812 ± 0.0017 $0.00046481 \pm 6.4753E-05$ 264.29 ± 2.200 0.01215 ± 0.00072528 1.771 ± 0.0033 0.01582 ± 0.00047544 $0.0001 \pm 4.4125E-05$ 250.04 ± 2.031 $0.00010934 \pm 0.00011648$ 234.66 ± 4.321 0.01410 ± 0.00086788 1.748 ± 0.0018 $0.00024037 \pm 3.8149E-05$ 243.56 ± 1.855 0.01187 ± 0.00030339 1.750 ± 0.00070073 Illipsometry model parameters and physical parameters. $0.00037490 \pm 8.7671E-05$ 180.05 ± 1.495 0.01111 ± 0.00075945 1.749 ± 0.0012 Model/Oscillator Thickness (nm)

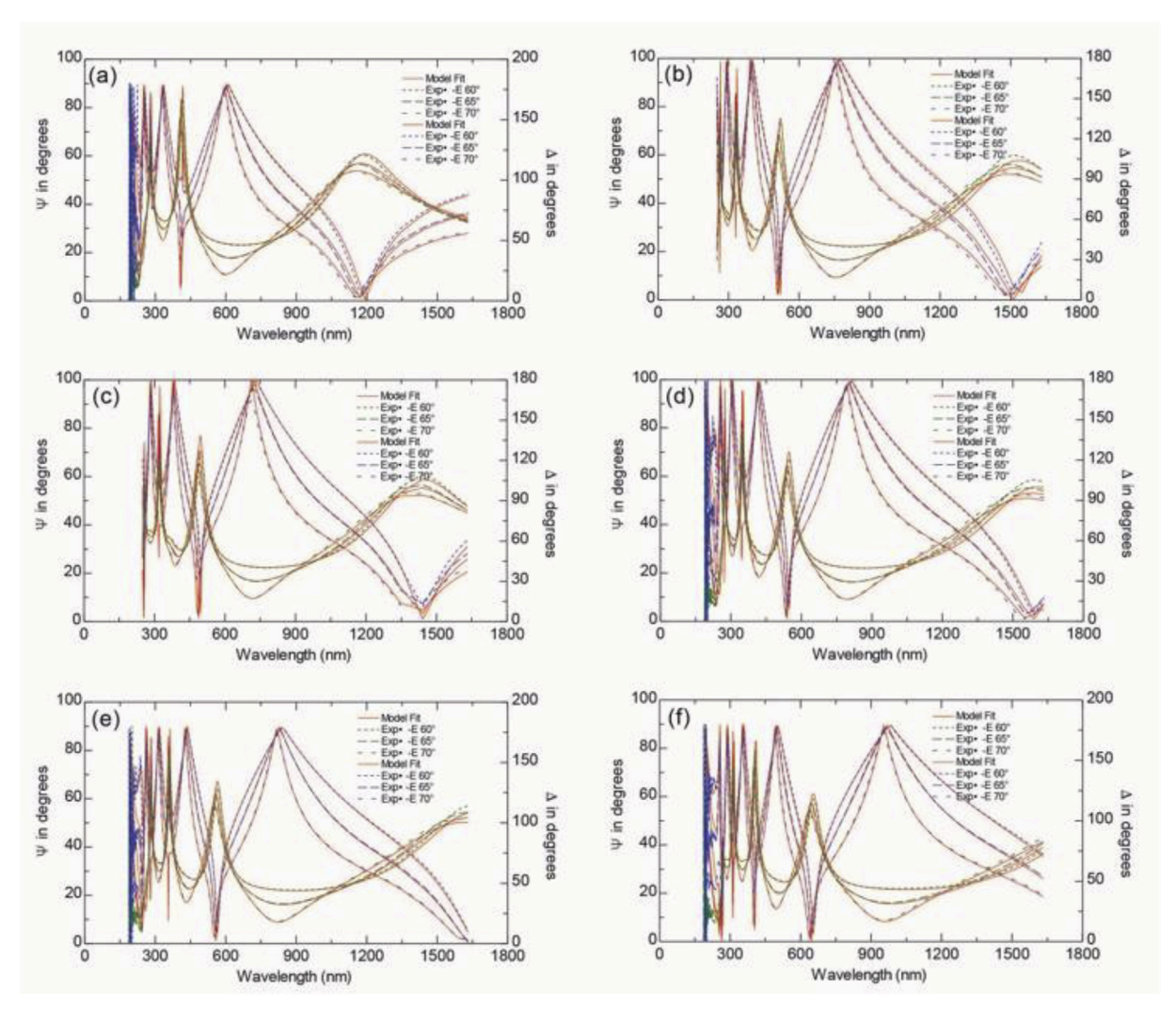


Fig. 2. Spectral dependence of Ψ and Δ for GTO films. The experimental and modelling curves are shown. The data of GTO films with variable sputtering power to the Ti target are shown in a (GTO-0), b (GTO-20), c (GTO-40), d (GTO-60), e (GTO-80), and f (GTO-1000), respectively.

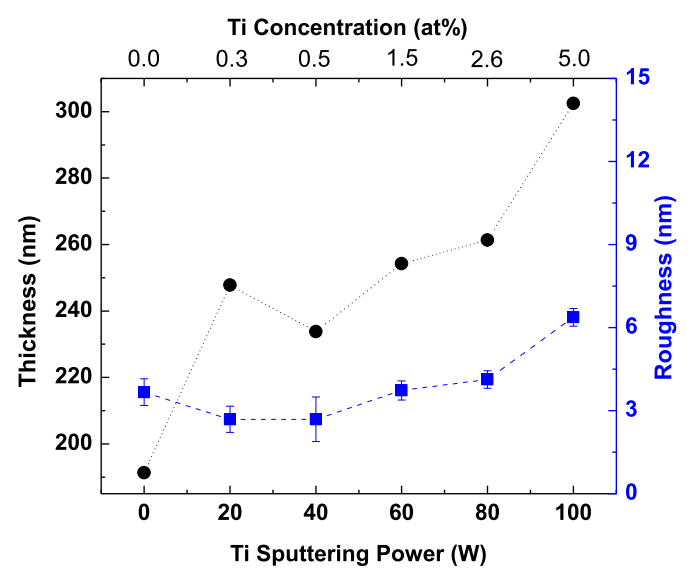
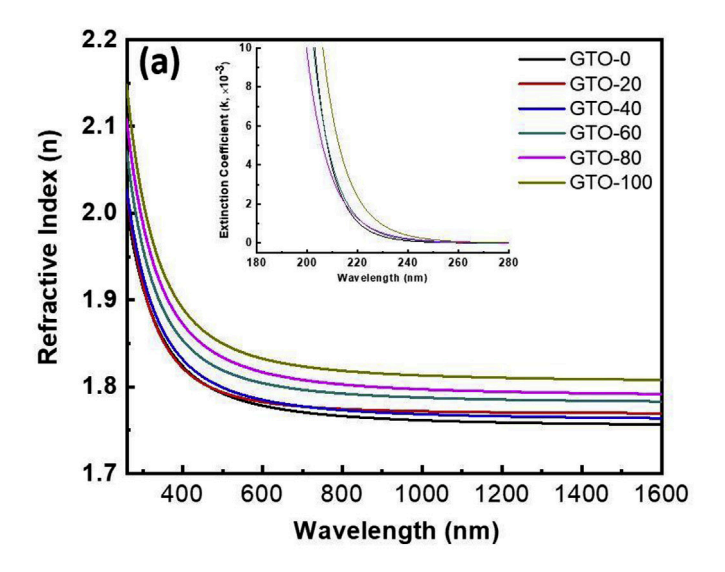


Fig. 3. Thickness and roughness variation of Ti doped Ga_2O_3 films. Circles represent the thickness values while squares represent the roughness values.

(Fig. 4a) indicate that the k value of the Ti-doped Ga_2O_3 films is almost zero in the visible and near-infrared spectral regions, while for photon energies toward the ultraviolet region, the extinction coefficient increases sharply. The $k(\lambda)$ behavior is obviously related to the optical quality of the films. Strong absorption with no weak shoulders or tailing behavior for the Ti-doped Ga_2O_3 films can be attributed to their high quality with a very high transparency, which was also confirmed by the spectrophotometry analysis of films [13]. Rapid increase in k values indicate the strong absorption across the band gap.

The structure and chemistry of the GTO films as a function of Ti content explains the functional dependence of optical constants on Ticontent. . Note that, for thin films and nanomaterials, the optical constants are sensitive to the microstructure and chemistry [20,22,31-33]. It is widely accepted that the surface/interface structure, crystal quality, packing density, lattice parameters, and defect structure strongly influences the optical parameters [3,20,22,25,27,29,31-34]. Thus, the Ti incorporation induced changes in the n-values and their dispersion profiles are directly correlated to the nanometric structure and chemistry of the GTO films. The good optical quality of the intrinsic Ga2O3 films (without any Ti) is due to their nanocrystalline structure and chemical stoichiometry, as indicated by the structural and chemical characterization. Usually, the low-packing density and/or stoichiometric defects can result in relatively low-values of optical constants compared to the bulk of the crystalline materials [25,29,34]. For instance, the optical constants of wide band gap HfO2 and Y2O3 films



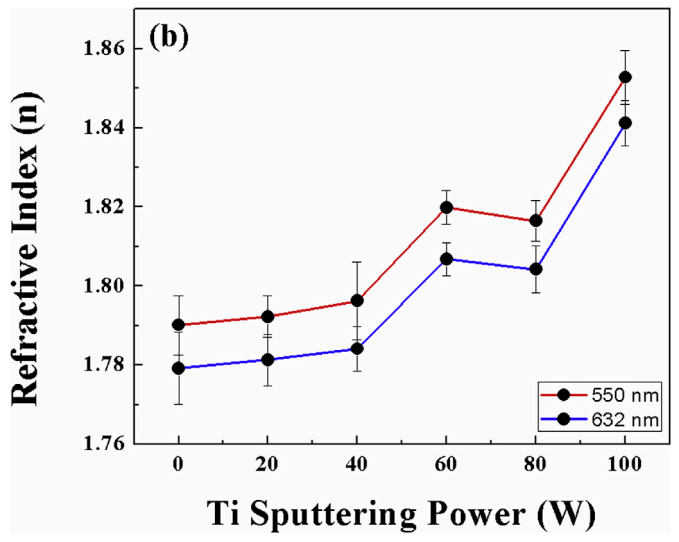


Fig. 4. a) Refractive index (*n*) dispersion profiles of GTO samples; b) Variation of '*n*' values of GTO samples at different two wavelength. Ti-induced increase in *n* values is evident.

were strongly influenced by their structural quality [25,29]; amorphous HfO_2 and Y_2O_3 films were found to exhibit low values of n and k which are explained on the basis of the structural disorder and low packing density in the amorphous matrix [25,29]. Thus, the good optical quality in terms of n and k values in $nc-Ga_2O_3$ films is attributed to the nanostructure, which is characterized by dense, randomly oriented nanocrystals. This leads to enhancement in packing density, which results in enhanced index of refraction. The additional evidence for the proposed mechanism comes from our earlier reports on the optical properties of nanocrystalline Y_2O_3 [25] and HfO_2 [29] films and other reports existing in the literature [27,32,34]. Furthermore, such behavior was also noticed in nanocrystalline Y_2O_3 [35] and Y_2O_3 [36]. Thus, the increased Y_2O_3 in Y_2O_3 [36] and Y_2O_3 [37] and Y_2O_3 [38] and Y_2O_3 [38] and Y_2O_3 [39] and Y_2O_3 [30] and Y

As to chemical composition changes, the refraction variation mechanisms seems to be dominant in Ti-doped Ga_2O_3 . It is known that Ti^{4+} ion has a very high refraction and, respectively, the substitution of " TiO_2 " for " Ga_2O_3 " could increase the refractive index. The examples of such analysis of several doped crystals could be found elsewhere [37–39]. Perhaps, the dominance of Ti induced chemical effects are more pronounced than structural effects to induce enhancement in n values. Based on the results reported in the literature on the optical

quality of CeO2 [36], HfO2 [29] and Y2O3 [25] films, one would expect to see a decrease in the n-values with progressive Ti content in GTO films. This is due to the fact that the structural characterization employing XRD and SEM analyses indicate that Ti-incorporation induces structural changes, where nanocrystalline GTO films eventually becomes amorphous at higher Ti content. However, the observed trend i.e., n-value increase with Ti, is primarily due to the chemical changes leading to the formation of Ga₂O₃-TiO₂ composite. While the detailed structural characterization is reported elsewhere [13], a brief summary of the results in the context of understanding the present work on optical constants variation with Ti doing is as follows. The GTO films exhibit the thermodynamically stable and single-phase β-Ga₂O₃ for lower Ti-content. However, structural transformation from crystalline to nearly amorphous state occurs with increasing Ti. Higher end of Ti content (~5 at%) results in the formation of Ga₂O₃-TiO₂ composite, where the amorphization of the Ga-Ti-O films was due to the TiO2 generation. The Ga₂O₃-TiO₂ composite formation was evident in both crystal structure and chemical composition analyses. Thus, the observed behavior in the optical constants of GTO films can be understood based on the chemical changes. The index of refraction of TiO2 is higher compared to that of Ga₂O₃. Therefore, increasing sputtering power to the Ti target results in higher Ti content, which is responsible for Ga₂O₃-TiO₂ composite formation and hence the overall enhancement in n values. Furthermore, such Ti-incorporation facilitated Ga₂O₃-TiO₂ composite formation may also be affecting the physical density of the films which in turn contribute to the *n*-enhancement. In order to validate this hypothesis we considered further analysis of the GTO optical data to determine the relative density of the films.

It is well known that the refractive index is closely related to the physical properties and density of the films [29,34,37]. Thus, the observed increase in refractive index of GTO films with addition of Ti may be due to increasing packing density of the films. In order to further confirm and validate this hypothesis, the relative density of the GTO films is calculated using Lorentz-Lorenz relationship. The Lorentz-Lorenz [40] equation is:

$$p = \frac{\rho_f}{\rho_b} = \frac{(n_f^2 - 1)(n_b^2 + 2)}{(n_f^2 + 2)(n_b^2 - 1)} \tag{7}$$

where p is the packing density, ρ_f is the density of the thin film, ρ_b is the density of the bulk material, n_f is mean refractive index of the film and n_b is the refractive index of the bulk material. The bulk refractive index (n_b) of $\beta\text{-}Ga_2O_3$ is 1.9201 [41,42] and the refractive index of the film measured at 550 nm is employed in Lorentz-Lorenz equation to calculate relative density of the film. The calculated relative density of GTO films is presented in Fig. 5. The physical density of GTO film increases with Ti content. Thus, the results and analysis of SE data confirm the density increase in Ti incorporated GTO films and accounts for the observed enhancement in n-values.

Finally, to understand the effect of Ti doping on the band gap (Eg) of Ga₂O₃ films, E_g values determined from SE are presented and compared with that of spectrophotometry analyses in Fig. 6. The E_g trend with Ti content is evident in Fig. 6. The E_g value for intrinsic Ga₂O₃ (without Ti incorporation) determined from absorption data is 5.40 (\pm 0.03) eV, which then continuously decreases to 4.41 (\pm 0.03) eV with increasing Ti content in the films. The effect of Ti doping and the physics and chemistry of the electronic structure changes leading to a substantial red shift in E_g can be understood as follows. We first consider the crystallographic data of Ga and Ti oxides separately, and we then consider the Ti doping-induced changes in the crystal structure of Ga₂O₃. Most important to note is the fact that both Ga₂O₃ and TiO₂ exhibit polymorphism. While Ti oxide exhibits rutile or anatase phases routinely, the monoclinic structure is thermodynamically favorable for Ga₂O₃ [20,43]. If the ionic size and other structural parameters are compatible or comparable, a solid solution without any structural change can be expected for Ti doping into a Ga₂O₃ lattice, i.e., Ti atoms

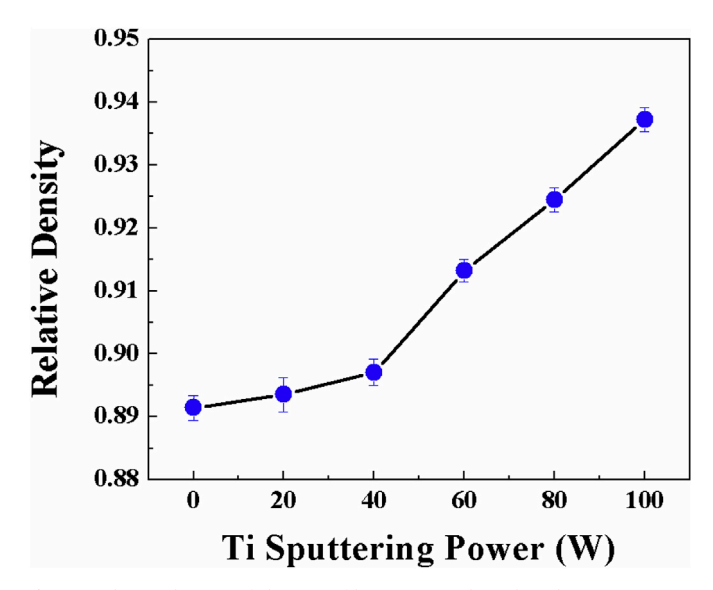


Fig. 5. Relative density of the GTO films. It is evident that the increasing Ti content improves the physical density of the GTO films.

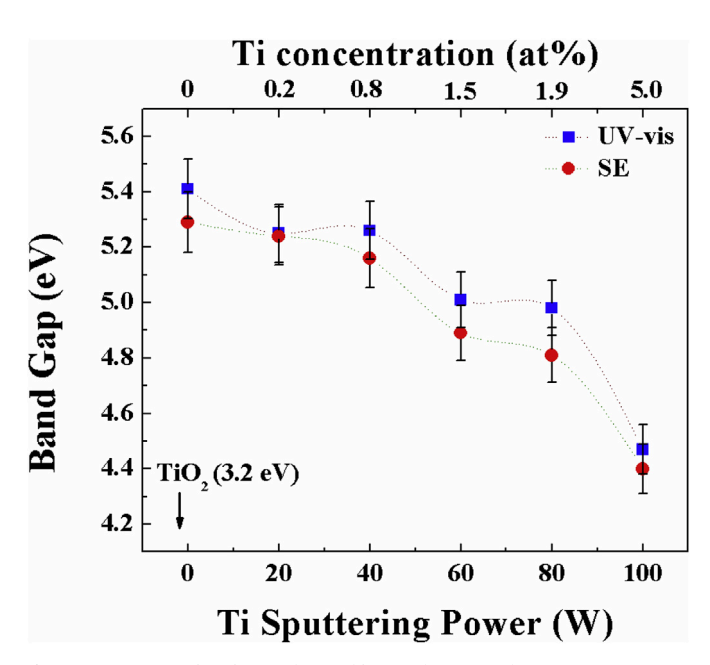


Fig. 6. Variation in band gap of GTO films as function of Ti sputtering power. The linked top X-axis shows the Ti at% determined from chemical analyses. For comparison, the data determined from spectrophotometry analysis [13] is also included. A direct correlation between $E_{\rm g}$ and Ti content can be seen.

can occupy the lattice positions of Ga inside the β-phase Ga_2O_3 . In fact, no evidence of a secondary phase or peak distortion for the parent β- Ga_2O_3 is seen in crystal structure analyses [13] when Ti concentration is ≤ 1.5 at%. Therefore, for the set of conditions employed in this work, the Ti-doped Ga_2O_3 films accommodate Ti without any structural distortion up to 1.5 at%, at which point the onset of Ti-induced changes result in the composite formation, as seen in the chemical analyses [13]. The reason for the Ti– Ga_2O_3 single phase system could be the comparable ionic radii of Ga^{3+} and Ti^{4+} ions, which are 0.062 nm and 0.069 nm, respectively [44]. Therefore, Ti ions can occupy the Ga_2O_3 structure without any perturbation only up to a certain limit. Exceeding this limit might result in Ti occupying interstitial positions, leading to changes in crystallography. Important to note that, as shown in Fig. 6, is $E_g \sim 3.2$ eV for Ti oxide (TiO₂) [13]. The measured E_g is not even close to this value, which is an indication of the composite film being

predominantly Ga_2O_3 in the matrix, while the presence of TiO_2 may be only as a minor component.

5. Conclusions

The effect of Ti doping on the optical characteristics, namely the index of refraction, optical absorption coefficient, and band gap, of nanocrystalline Ga₂O₃ films were investigated in detail using spectroscopic ellipsometry. The results shed light on the optical behavior of Tidoped Ga₂O₃ films, where the Ti-induced changes are visible in terms of the dispersion profiles of n and k and the E_g -composition dependence. The E_g value decreases significantly to ~4.2 eV for the 5 at% of Ti doped Ga₂O₃ films. The n values at 632 nm increases from 1.78 to 1.84 with increasing Ti concetration from 0 to ~ 5 at%. The *n*-value enhancement with Ti is attributed to the Ga2O3-TiO2 composite formation, where the chemical changes i.e., a composite formation, are more dominant than the structural changes i.e., amorphization of the Ga-Ti-O films with increasing Ti content. Titanium doping induced Ga₂O₃-TiO₂ composite formation successfully accounts for the n-enhancement and E_g-reduction in transparent GTO films. Additionally, Lorentz-Lorenz analysis of the ellipsometry data indicates the gradual improvement in the packing density coupled with structural transformation accounts for the observed optical quality of the Ti-doped Ga₂O₃ films. A correlation established between the structure, Ti-concentration and optical constants of GTO films may be useful and provide a road-map for their effective integration in practical optical and optoelectronic devices.

Declaration of interests

The authors declare that they have no known competing financial interests or personal relationships that could have appeared to influence the work reported in this paper.

Author contributions and statement

CVR conceived and supervised the research. SM and AKB deposited the samples and fabricated GTO films on Si(100) for ellipsometry studies. SM, AKB, CO and CVR characterized the samples. CVR coordinated the project and scientific contributions from all the authors. All authors were involved in data analyses, designed figures, and wrote the manuscript. CVR coordinated to collect the comments and feedback from all co-authors. Finally, all the authors approved the submission.

Acknowledgements

The authors acknowledge, with pleasure, support from the National Science Foundation with NSF-PREM grant #DMR-1827745.

Appendix A. Supplementary data

Supplementary data to this article can be found online at https://doi.org/10.1016/j.optmat.2019.109223.

References

- [1] S.J. Pearton, J. Yang, P.H. Cary, F. Ren, J. Kim, M.J. Tadjer, M.A. Mastro, A review of Ga₂O₃ materials, processing, and devices, Appl. Phys. Rev. 5 (2018) 011301.
- 2] E.J. Rubio, T.E. Mates, S. Manandhar, M. Nandasiri, V. Shutthanandan, C.V. Ramana, Tungsten incorporation into gallium oxide: crystal structure, surface and interface chemistry, thermal stability, and interdiffusion, J. Phys. Chem. C 120 (2016) 26720–26735.
- [3] E.J. Rubio, C.V. Ramana, Tungsten-incorporation induced red-shift in the bandgap of gallium oxide thin films, Appl. Phys. Lett. 102 (2013) 191913.
- [4] M. Fleischer, L. Höllbauer, H. Meixner, Effect of the sensor structure on the stability of Ga₂O₃ sensors for reducing gases, Sens. Actuators B 18 (1994) 119–124.
- [5] D. Guo, Y. An, W. Cui, Y. Zhi, X. Zhao, M. Lei, L. Li, P. Li, Z. Wu, W. Tang, Epitaxial growth and magnetic properties of ultraviolet transparent Ga₂O₃/(Ga_{1-x}Fe_x)₂O₃ multilayer thin films, Sci. Rep. 6 (2016) 25166.
- [6] D. Guo, P. Li, Z. Wu, W. Cui, X. Zhao, M. Lei, L. Li, W. Tang, Inhibition of

unintentional extra carriers by Mn valence change for high insulating devices, Sci. Rep. 6 (2016) 24190.

- [7] X.Z. Liu, P. Guo, T. Sheng, L.X. Qian, W.L. Zhang, Y.R. Li, β-Ga₂O₃ thin films on sapphire pre-seeded by homo-self-templated buffer layer for solar-blind UV photodetector, Opt. Mater. 51 (2016) 203–207.
- [8] Wei Mi, Caina Luan, Zhao Li, Cansong Zhao, Xianjin Feng, Jin Ma, Ultraviolet–green photoluminescence of β -Ga₂O₃ films deposited on MgAl₆O₁₀ (1 0 0) substrate, Opt. Mater. 35 (2013) 2624–2628.
- [9] L.-X. Qian, Z.-H. Wu, Y.-Y. Zhang, P.T. Lai, X.-Z. Liu, Y.-R. Li, Ultrahigh-responsivity, rapid-recovery, solar-blind photodetector based on highly nonstoichiometric amorphous gallium oxide, ACS Photonics 4 (2017) 2203–2211.
- [10] S.H. Lee, S.B. Kim, Y.-J. Moon, S.M. Kim, H.J. Jung, M.S. Seo, K.M. Lee, S.-K. Kim, S.W. Lee, High-responsivity deep-ultraviolet-selective photodetectors using ultrathin gallium oxide films, ACS Photonics 4 (2017) 2937–2943.
- [11] W. Xu, H. Cao, L. Liang, J.B. Xu, Aqueous solution-deposited gallium oxide dielectric for low-temperature, low-operating-voltage indium oxide thin-film transistors: a facile route to green oxide electronics, ACS Appl. Mater. Interfaces 7 (2015) 14720–14725.
- [12] I. López, E. Nogales, B. Méndez, J. Piqueras, A. Peche, J. Ramírez-Castellanos, J.M. González-Calbet, Influence of Sn and Cr doping on morphology and luminescence of thermally grown Ga₂O₃ nanowires, J. Phys. Chem. C 117 (2013) 3036–3045.
- [13] S. Manandhar, C.V. Ramana, Direct, functional relationship between structural and optical properties in titanium-incorporated gallium oxide nanocrystalline thin films, Appl. Phys. Lett. 110 (2017) 061902.
- [14] A.K. Battu, S. Manandhar, C.V. Ramana, Molybdenum incorporation induced enhancement in the mechanical properties of gallium oxide films, Adv. Mater. Interfaces 4 (2017) 1700378.
- [15] A.K. Battu, S. Manandhar, V. Shutthanandan, C.V. Ramana, Controlled optical properties via chemical composition tuning in molybdenum-incorporated β-Ga₂O₃ nanocrystalline films, Chem. Phys. Lett. 684 (2017) 363–367.
- [16] W. Zhang, B.S. Naidu, J.Z. Ou, A.P. O'Mullane, A.F. Chrimes, B.J. Carey, Y. Wang, S.Y. Tang, V. Sivan, A. Mitchell, S.K. Bhargava, K. Kalantar-Zadeh, Liquid metal/metal oxide frameworks with incorporated Ga₂O₃ for photocatalysis, ACS Appl. Mater. Interfaces 7 (2015) 1943–1948.
- [17] X. Wang, S. Shen, S. Jin, J. Yang, M. Li, X. Wang, H. Han, C. Li, Effects of Zn2+ and Pb2+ dopants on the activity of Ga₂O₃-based photocatalysts for water splitting, Phys. Chem. Chem. Phys. 15 (2013) 19380–19386.
- [18] Y. Sakata, Y. Matsuda, T. Yanagida, K. Hirata, H. Imamura, K. Teramura, Effect of metal ion addition in a Ni supported Ga₂O₃ photocatalyst on the photocatalytic overall splitting of H₂O. Catal. Lett. 125 (2008) 22–26.
- overall splitting of H₂O, Catal. Lett. 125 (2008) 22–26.

 [19] W. Zhang, J.Z. Ou, S.-Y. Tang, V. Sivan, D.D. Yao, K. Latham, K. Khoshmanesh, A. Mitchell, A.P. O'Mullane, K. Kalantar-zadeh, Liquid metal/metal oxide frameworks, Adv. Funct. Mater. 24 (2014) 3799–3807.
- [20] S.S. Kumar, E.J. Rubio, M. Noor-A-Alam, G. Martinez, S. Manandhar, V. Shutthanandan, S. Thevuthasan, C.V. Ramana, Structure, morphology, and optical properties of amorphous and nanocrystalline gallium oxide thin films, J. Phys. Chem. C 117 (2013) 4194–4200.
- [21] J. Woollam, Guide to Using WVASE32 Spectroscopic Ellipsomtry Data Acquisition and Analysis Software, JA Woollam Co, in, Inc, 2005.
- [22] G.E. Jellison, The calculation of thin film parameters from spectroscopic ellipsometry data, Thin Solid Films 290–291 (1996) 40–45.
- [23] H. Fujiwara, Spectroscopic Ellipsometry: Principles and Applications, John Wiley & Sons, 2007.
- [24] C.V. Ramana, S. Utsunomiya, R.C. Ewing, U. Becker, V.V. Atuchin, V.S. Aliev,

- V.N. Kruchinin, Spectroscopic ellipsometry characterization of the optical properties and thermal stability of ZrO₂ films made by ion-beam assisted deposition, Appl. Phys. Lett. 92 (2008) 011917.
- [25] V.H. Mudavakkat, V.V. Atuchin, V.N. Kruchinin, A. Kayani, C.V. Ramana, Structure, morphology and optical properties of nanocrystalline yttrium oxide (Y₂O₃) thin films, Opt. Mater. 34 (2012) 893–900.
- [26] C.V. Ramana, E. Rubio, C. Barraza, A. Miranda Gallardo, S. McPeak, S. Kotru, J. Grant, Chemical bonding, optical constants, and electrical resistivity of sputterdeposited gallium oxide thin films, J. Appl. Phys. 115 (2014) 043508.
- [27] C.V. Ramana, R. Vemuri, V. Kaichev, V. Kochubey, A. Saraev, V. Atuchin, X-ray photoelectron spectroscopy depth profiling of La₂O₃/Si thin films deposited by reactive magnetron sputtering, ACS Appl. Mater. Interfaces 3 (2011) 4370–4373.
- [28] M. Vargas, N.R. Murphy, C.V. Ramana, Tailoring the index of refraction of nanocrystalline hafnium oxide thin films, Appl. Phys. Lett. 104 (2014) 101907.
- [29] M. Vargas, N.R. Murphy, C.V. Ramana, Structure and optical properties of nanocrystalline hafnium oxide thin films, Opt. Mater. 37 (2014) 621–628.
- [30] T. Tan, Z. Liu, H. Lu, W. Liu, H. Tian, Structure and optical properties of HfO₂ thin films on silicon after rapid thermal annealing, Opt. Mater. 32 (2010) 432–435.
- [31] B. Keswani, R. Devan, R. Kambale, A.R. James, S. Manandhar, Y. Kolekar, C.V. Ramana, Correlation between structural, magnetic and ferroelectric properties of Fe-doped (Ba-Ca)TiO₃ lead-free piezoelectric, J. Alloy. Comp. 712 (2017) 320–333.
- [32] I. Kosacki, V. Petrovsky, H.U. Anderson, Band gap energy in nanocrystalline ZrO₂:16%Y thin films, Appl. Phys. Lett. 74 (1999) 341–343.
- [33] S. Krishnamoorthy, Z. Xia, C. Joishi, Y. Zhang, J. McGlone, J. Johnson, M. Brenner, A.R. Arehart, J. Hwang, S. Lodha, S. Rajan, Modulation-doped β-(Al_{0.2}Ga_{0.8})₂O₃/ Ga₂O₃ field-effect transistor, Appl. Phys. Lett. 111 (2017) 023502.
- [34] R.S. Vemuri, M.H. Engelhard, C.V. Ramana, Correlation between surface chemistry, density, and band gap in nanocrystalline WO₃ thin films, ACS Appl. Mater. Interfaces 4 (2012) 1371–1377.
- [35] G. Malandrino, M. Blandino, M.E. Fragala, M. Losurdo, G. Bruno, Relationship between nanostructure and optical properties of ZnO thin films, J. Phys. Chem. C 112 (2008) 9595–9599.
- [36] R.G. Toro, G. Malandrino, I.L. Fragalà, R. Lo Nigro, M. Losurdo, G. Bruno, Relationship between the nanostructures and the optical properties of CeO_2 thin films, J. Phys. Chem. B 108 (2004) 16357–16364.
- [37] V. Atuchin, C. Ziling, I. Savatinova, M. Armenise, V. Passaro, Waveguide formation mechanism generated by double doping in ferroelectric crystals, J. Appl. Phys. 78 (1995) 6936–6939.
- [38] V. Atuchin, C. Ziling, D. Shipilova, N. Beizel, Crystallographic, ferroelectric and optical properties of TiO₂-doped LiNbO₃ crystals, Ferroelectrics 100 (1989) 261–269.
- [39] A. Korotkov, V. Atuchin, Prediction of refractive index of inorganic compound by chemical formula, Optic Commun. 281 (2008) 2132–2138.
- [40] N. Kaiser, Optical Interference Coatings, 1 ed., Springer-Verlag Berlin Heidelberg, 2003.
- [41] S. Stepanov, V. Nikolaev, V. Bougrov, A. Romanov, Gallium oxide: properties and applications- a review, Rev. Adv. Mater. Sci. 44 (2016) 63–86.
- [42] I. Bhaumik, R. Bhatt, S. Ganesamoorthy, A. Saxena, A.K. Karnal, P.K. Gupta, A.K. Sinha, S.K. Deb, Temperature-dependent index of refraction of monoclinic Ga₂O₃ single crystal, Appl. Opt. 50 (2011) 6006–6010.
- [43] M. Yamaga, E.G. Víllora, K. Shimamura, N. Ichinose, M. Honda, Donor structure and electric transport mechanism in β Ga_2O_3 , Phys. Rev. B 68 (2003) 3135–3144.
- [44] R.D. Shannon, Revised effective ionic radii and systematic studies of interatomic distances in halides and chalcogenides, Acta Crystallogr. A 32 (1976) 751–767.